Vacuum 118 (2015) 32–37

Contents lists available at ScienceDirect

Vacuum

journal homepage: www.elsevier.com/locate/vacuum

Dependence of performance parameters of CdTe solar cells on semiconductor properties studied by using SCAPS-1D

Chia-Hua Huang*, Wen-Jie Chuang

Department of Electrical Engineering, National Dong Hwa University, No. 1, Section 2, University Road, Shou-Feng, Hualien 97401, Taiwan

ARTICLE INFO

Article history:
Received 30 July 2014
Received in revised form
4 March 2015
Accepted 7 March 2015
Available online 20 March 2015

Keywords:
CdTe solar cells
Defect density
Carrier concentration
Carrier mobility

ABSTRACT

A baseline model and an advanced model of CdTe solar cells with selected semiconductor properties fit to the performance parameters of the champion CdTe solar cells were developed. The responsible factors for the efficiency improvement of high-performance CdTe solar cell were analyzed. The thin CdS films, and the low defect densities and high carrier mobilities of the CdS films were the crucial factors for the enhancement of the short-circuit current density. With the suppression of carrier recombination, the open-circuit voltage and fill factor of the CdTe solar cells with the low defect densities in either CdTe films or interdiffusion layer were enhanced. In addition, the carrier collection was impeded for the interdiffusion layer with a high defect density, leading to the decrease of the short-circuit current density. Moreover, the simulation results revealed that the efficiency of 20–21% was achieved for the CdTe solar cells with the low defect densities and high carrier concentrations of CdTe films.

1. Introduction

Cadmium telluride (CdTe) is one of the promising materials for low-cost and high-efficiency photovoltaic devices due to its features of direct band-gap well matching the solar spectrum of AM 1.5G, the high absorption coefficients of around 10^5 cm^{-1}, and the theoretical efficiency reaching around 29% [1]. The previous best efficiency records of around 16% for CdTe solar cells were held for nearly one decade until the significant improvements in efficiency were contributed from First Solar and General Electric (GE) Global Research in recent years [2–7]. For the confirmed efficiency records measured under the standard reporting conditions of AM 1.5G (1000 W/m^2) at 25 °C, the CdTe solar cells have reached the efficiency of 19.6% in 2013, where the circuit-short current density (J_{SC}) is 28.6 mA/cm^2 [6]. First Solar reported a conversion efficiency of 20.4%, which was recognized as a 'notable exception', in early 2014 [7]. The efficiency of CdTe solar cells have even advanced to 21.0% in mid 2014 [8]. In addition, the CdTe modules have even reached an aperture-area efficiency of 17.5%, which is best thin-film module record [7]. The considerable progress has been made for the CdTe photovoltaic technologies. A better understanding and analysis of the fundamental issues about the efficiency improvement would be favorable to further optimize the performance of the CdTe solar cells.

A variety of studies on the device modeling of CdTe solar cells has been conducted previously. The researches about how the carrier lifetimes, carrier densities, back contact barriers, CdTe film thickness, and electron reflector impacting the characteristics of CdTe solar cells were reported [9–14]. In order to identify the mechanisms for the improvement of CdTe solar cells, a study of the numerical modeling and device simulations to investigate the critical factors governing the performance of CdTe solar cells was carried out. By using the approach of device simulations, the intention was to explore and provide the responsible routes for the efficiency improvement from 16.4% [3] to 19.6% [6] in terms of semiconductor properties or device physics. A baseline device model and an advanced model with the superior semiconductor properties for the CdTe solar cells were constructed. With the selection of reasonable input parameters, the simulation results of the baseline device model and advanced model were fit to the experimental data of performance parameters for the confirmed efficiency records of 16.4% and 19.6%, respectively. The dominant factors for the efficiency improvement are presented and analyzed. Moreover, the potential paths for the further improvements of efficiency beyond 21% are proposed.

* Corresponding author. Tel.: +886 3 8634077.
E-mail address: chuang@mail.ndhu.edu.tw (C.-H. Huang).

http://dx.doi.org/10.1016/j.vacuum.2015.03.008
0042-207X/

2. Device modeling

The baseline device structure of CdTe solar cells used in the simulation consisted of SnO_2 layer, CdS layer, CdTe absorber, and bottom contact. The computer simulation tool, Solar Cell Capacitance Simulator – 1 Dimension (SCAPS-1D) [15,16], was employed for the simulations. To proceed with the simulations, the material parameters employed as the inputs were selected based on the reported literature values or confined to reasonable ranges. The key semiconductor properties of the SnO_2 layer, CdS layer, and CdTe absorber as the input parameters for the simulations are given in Table 1. The total thickness of the absorber layer was maintained at 4 μm for all cases. A deep defect level was located in the middle of band-gap as an effective recombination center for each layer of the device structure.

An interdiffusion layer of $CdTe_{1-x}S_x$ compound, resulting from the diffusion of CdS and CdTe during the fabrication processes of the heat treatment or $CdCl_2$ treatment, formed between the CdS and CdTe layers has been reported [17,18]. The interdiffusion layer was incorporated in the device model. Referred to the distribution of carrier density within the interdiffusion layer reported in the literature [19], the interdiffusion layer had a donor concentration varying exponentially form 10^{17} cm^{-3} near CdS side down to 10^{13} cm^{-3} near CdTe bulk, and a background acceptor concentration of 2×10^{14} cm^{-3}. The band-gap energy of $CdTe_{1-x}S_x$ was determined from the equation reported in the literature with the band-gap energy of 1.45 eV for CdTe and estimated x ~ 0.05 [1,20].

3. Results and discussion

3.1. Baseline model and advanced model

For the baseline model of CdTe solar cells, the cell structure consisted of the TCO (transparent conductive oxide), CdS, and CdTe layers. The input parameters are given in Table 1. The majority of input parameters for the simulations were adopted from reported literature [21,22]. Constrained to the more reasonable ranges of the experimental data for the typical CdTe solar cells, the thickness of 70 nm, the defect density of 5×10^{16} cm^{-3}, the hole mobility of 10 cm^2 V^{-1} s^{-1}, and the electron mobility of 40 cm^2 V^{-1} s^{-1} for the CdS layer of the CdTe solar cells were employed for the simulations. Furthermore, these input parameters were especially selected to fit the performance parameters to the previous best performance record of 16.4% [3]. The results are shown in Fig. 1.

With the consideration of the interdiffusion between the CdS and CdTe layers, an interdiffusion layer was incorporated in the advanced model of the CdTe solar cells. The cell structure of the advanced model is exhibited in Fig. 2. Fitting the best efficiency record of 19.6% [6] and the external quantum efficiency (EQE) for the short-circuit current density of 28.6 mA/cm^2 reported for the CdTe solar cells [23], the advanced model with the improved properties of CdS and CdTe semiconductors was developed. In contrast to the baseline model, the thickness of CdS layer was thin, and the carrier mobilities of CdS film were enhanced for the

Table 1
Simulation parameters for the baseline model of CdTe solar cells with an efficiency of 16.4%.

Layer properties	SnO_2	CdS	CdTe
Thickness (nm)	500	70	4000
$\varepsilon/\varepsilon_0$	9	10	9.4
E_g (eV)	3.6	2.4	1.45
N_c (cm^{-3})	4×10^{18}	2.2×10^{18}	8.0×10^{17}
N_v (cm^{-3})	2×10^{19}	1.8×10^{19}	1.8×10^{19}
μ_n (cm^2 V^{-1} s^{-1})	100	40	320
μ_p (cm^2 V^{-1} s^{-1})	25	10	40
n or p (cm^{-3})	n: 10^{18}	n: 10^{17}	p: 2×10^{14}

$\varepsilon/\varepsilon_0$: relative permittivity; E_g: band-gap energy; N_c: effective density of states in conduction band; N_v: effective density of states in valance band; μ_n: electron mobility; μ_p: hole mobility; n: donor density; p: acceptor density.

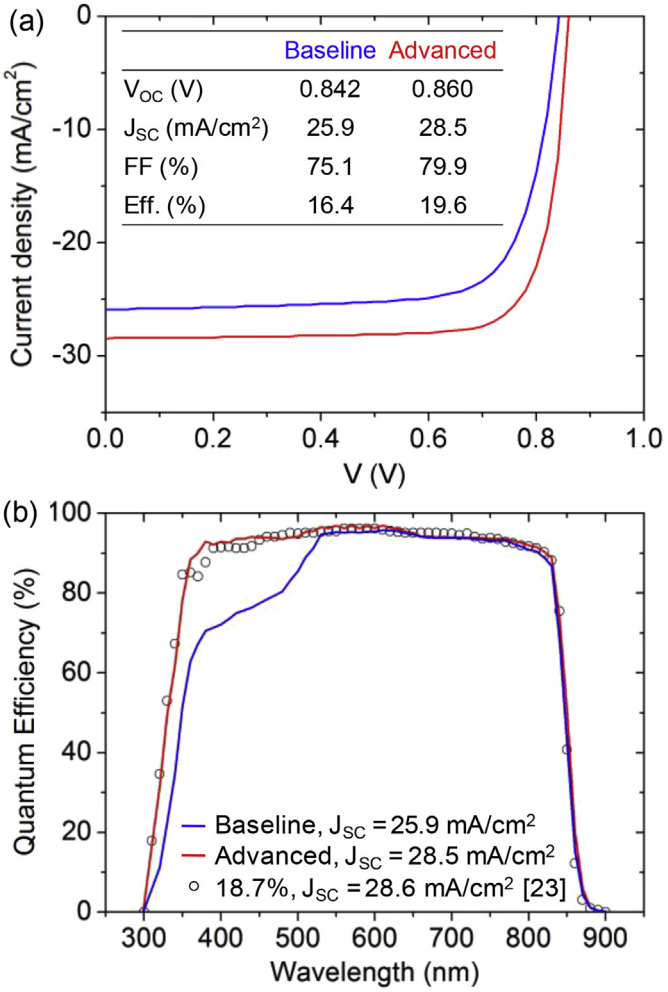

Fig. 1. (a) *J–V* curves and (b) external quantum efficiency of CdTe solar cells with simulation efficiencies of 16.4% and 19.6%.

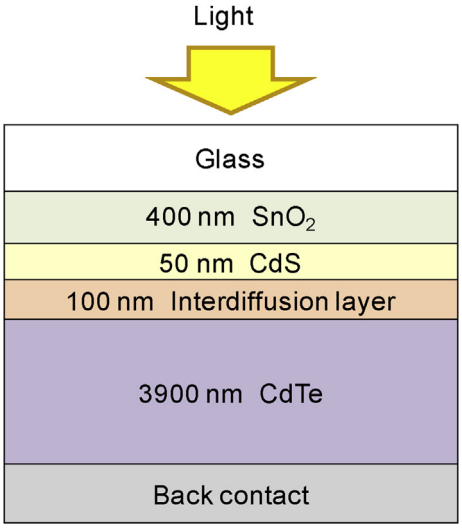

Fig. 2. Device structure of CdTe solar cells for the device simulations.

advanced model. Additionally the defect densities of both CdS and CdTe layers were lessened. The input parameters of this advanced model for the simulations are summarized in Table 2. The schematic energy-band diagram of the CdTe solar cell under the equilibrium condition is illustrated in Fig. 3, where E_C is the conduction band edge, E_V is the valence band edge, and E_F is the Fermi level. The current–voltage characteristics of *J–V* curves and the EQE of CdTe solar cells for the advanced model are shown in Fig. 1(a) and (b), respectively. The simulation efficiencies achieved for the advanced model of CdTe solar cells were enhanced. The main contribution of the efficiency improvement was attributed to the increase of short-circuit current density. Compared with the baseline model, there was an increase of about 10% for the short-circuit current density of the advanced model. The analysis of the EQE results for the baseline and advanced model, as shown in Fig. 1(b), demonstrated that the improvement of short-circuit current density resulted from the enhancement of EQE in the region of short wavelength below 520 nm. It is evident that the properties of CdS films were improved so that the EQE at short wavelengths was enhanced, leading to the improvement of short-circuit current density. Compared with the simulation results of the baseline model, the fill factor was moderately improved while the open-circuit voltage was slightly improved for the advanced model. The responsible factors for the improvement of fill factor and open-circuit voltage are discussed in detail as follows.

3.2. Analysis of critical factors impacting the performance of CdTe solar cells

As shown in Fig. 1(b), the EQE results indicated that the improvement of short-circuit current density resulted from the improved properties of CdS films including the reduced defect densities and enhanced carrier mobilities. Moreover, thin CdS films could also enhance the short-circuit current density. With the wider band-gap energy of CdS films than that of CdTe films, obviously thin CdS films resulted in more photons transmitting into CdTe films. Consequently, more photo-generated carriers were created in the CdTe films, and thus the short-circuit current density was improved. For the CdS layers with the thickness varying from 10 nm to 200 nm as illustrated in Fig 4(a), the greater EQE was achieved for the thinner CdS films. In addition, the EQE for the defect density of CdS films varying from 10^{15} cm^{-3} to 10^{18} cm^{-3} are shown in Fig. 4(b). The EQE increased for the defect density decreased from 10^{18} cm^{-3} to 10^{16} cm^{-3}, reaching its saturated value for the defect density below 10^{16} cm^{-3}. The carrier recombination was increased for the high defect densities of CdS films, resulting in the low EQE at the short wavelengths. Besides, the EQE at short wavelengths was improved for the CdS films with the greater carrier mobility, as shown in Fig. 4(c). The carrier collection was improved for the CdS films with the greater majority carrier mobility, resulting in the higher EQE and the enhanced short-circuit current density. The EQE nearly reached its saturated values for the carrier mobilities equal to or greater than 10 cm^2 V^{-1} s^{-1}.

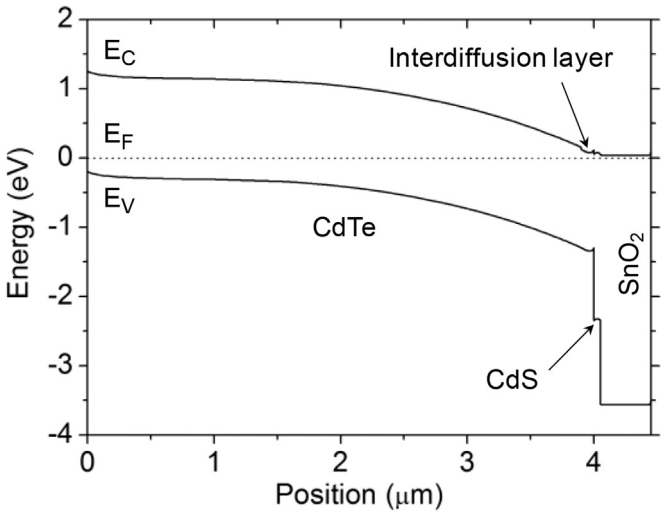

Fig. 3. Schematic band diagram of CdTe solar cells under equilibrium.

The dependence of the cell performance parameters on the thickness of CdS films with various carrier mobilities was further investigated, and the results for the CdS layers with the thickness varying from 10 nm to 200 nm are shown in Fig. 5. For the specified carrier mobilities of 10 cm^2 V^{-1} s^{-1} or 100 cm^2 V^{-1} s^{-1} for the CdS films, the short-circuit current density was slightly improved with the decrease of CdS film thickness. On the other hand, there was a stronger dependence of the short-circuit current density on the thickness of the CdS films with the lower carrier mobilities of 10^{-2} cm^2 V^{-1} s^{-1} to 1 cm^2 V^{-1} s^{-1}. The short-circuit current density was improved with the reduction of film thickness for the CdS layers with the relatively low carrier mobilities. The simulation results suggested that the great short-circuit current density could be achieved by simply reducing the film thickness of CdS layers regardless the other characteristics of CdS films. However, experimentally, a uniform coverage of the CdS layer on the CdTe film is required in order to take advantage of the thin CdS films.

Although the simulation results revealed that the characteristics of CdS films affected the short-circuit current density of CdTe solar cells, the variation of properties for the CdS layers had no remarkable impact on both the open-circuit voltage and fill factor of the CdTe solar cells as shown in Fig. 5. Thus, as illustrated in Fig. 5, the varying tendency of the conversion efficiency followed the varying trend of the short-circuit current density.

The improvement of fill factor and open-circuit voltage for the advanced model can be principally attributed to the decrease of defect density of CdTe films. As illustrated in Fig. 6, the performance parameters of CdTe solar cells deteriorated with the increase of the defect densities of CdTe films. The short-circuit current density

Table 2
Simulation parameters for the advanced model of CdTe solar cells with an efficiency of 19.6%.

Layer properties	SnO_2	CdS	Interdiffusion layer	CdTe
Thickness (nm)	400	50	100	3900
$\varepsilon/\varepsilon_0$	9	10	9.4	9.4
E_g (eV)	3.6	2.4	1.42	1.45
N_c (cm^{-3})	4×10^{18}	2.2×10^{18}	8.0×10^{17}	8.0×10^{17}
N_v (cm^{-3})	2×10^{19}	1.8×10^{19}	1.8×10^{19}	1.8×10^{19}
μ_n (cm^2 V^{-1} s^{-1})	100	80	320	320
μ_p (cm^2 V^{-1} s^{-1})	25	20	40	40
n or p (cm^{-3})	n: 10^{18}	n: 10^{17}	n: 10^{13}–10^{17} (exponential) p: 2×10^{14}	p: 2×10^{14}

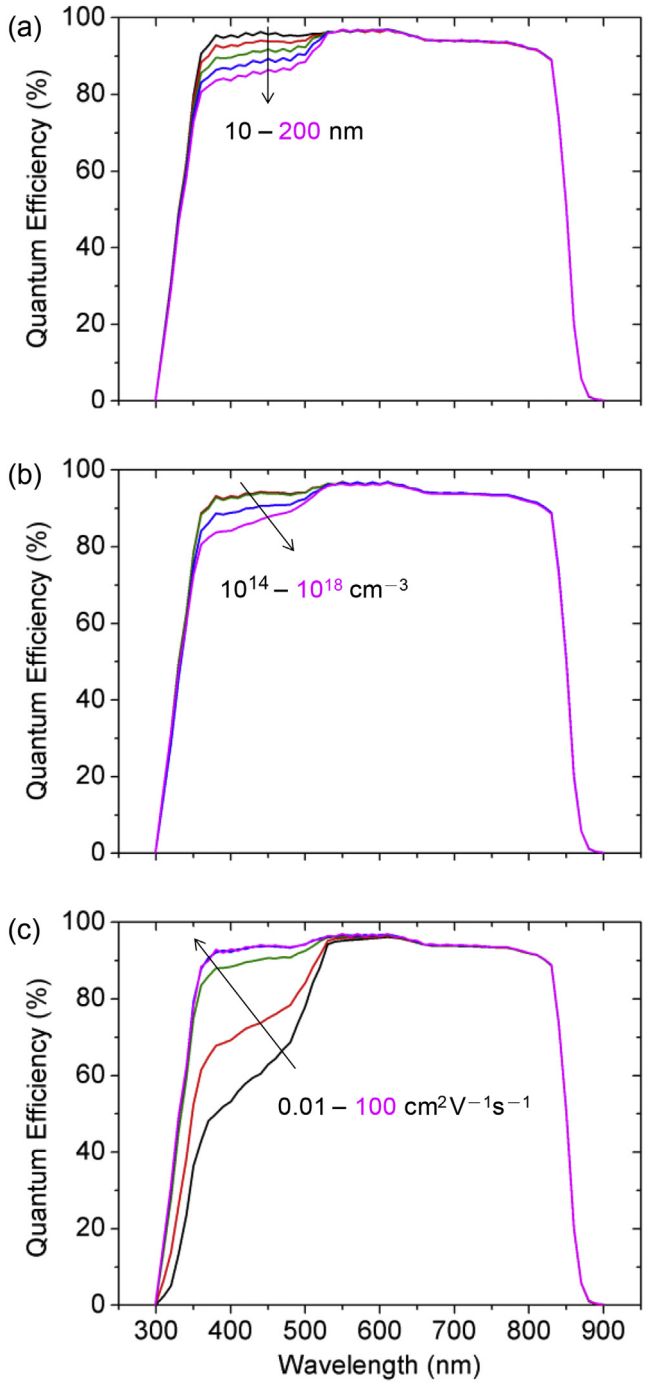

Fig. 4. Dependence of external quantum efficiency on (a) film thickness, (b) defect density, and (c) carrier mobility of CdS films for CdTe solar cells.

were nearly kept constant for the defect densities of CdTe films increased from 10^{12} cm^{-3} to 10^{14} cm^{-3}, and were slightly decreased for the defect densities increased to 10^{15} cm^{-3}. On the other hand, both the open-circuit voltage and fill factor decreased with the increase of the defect densities. With the low defect density, the carrier recombination within the CdTe films was suppressed, and thus the open-circuit voltage and fill factor were enhanced. A positive correlation between the open-circuit voltage as well as the fill factor of the CdTe solar cells and the defect densities of the CdTe films is evident.

As labeled in Fig. 6, when the defect density of CdTe films decreased from 2×10^{14} cm^{-3} to 7×10^{13} cm^{-3}, the corresponding open-circuit voltage increased from 0.846 V to 0.860 V, and the corresponding fill factor increased from 76.3% to 79.9%, where the improved rates of open-circuit voltage and fill factor were close to those of the advanced model as indicated in Fig. 1. Nevertheless, there was no substantial variation of short-circuit current density for the defect densities within this range of 7×10^{13} cm^{-3} to 2×10^{14} cm^{-3}. The reduction of defect density in CdTe films is considered to account for the enhancement of open-circuit voltage and fill factor of the CdTe solar cells.

The n-type interdiffusion layer could be beneficial to the diminishment of the carrier recombination rate around the junction by shifting the electrical junction away from the high-recombination hetero-interface between the CdS and the interdiffusion layer. With the incorporation of the interdiffusion layer in the CdTe solar cells, the defect density of the interdiffusion layer was employed as a variable to study its impacts on the performance of CdTe solar cells. The results are presented in Fig. 7. Due to the fact that most of the photo-generated carriers are near the surface region of the CdTe layers, the carrier collection efficiency of CdTe solar cells is expected to deteriorate for the surface region of the CdTe layers with a high density of recombination centers. Thus, the high defect density in the interdiffusion layer gave rise to the inefficient carrier collection, and hence the reduction of the short-circuit current density. Furthermore, for the interdiffusion layer with the low defect densities, the carrier collection was not only ameliorated but also the carrier recombination was restrained such that both the open-circuit voltage and fill factor were enhanced. Thus, the performance of CdTe solar cells was improved.

3.3. *Efficiency beyond 20%*

As shown in Fig. 6, the performance parameters approximately saturated when the defect densities of CdTe films dropped down to 10^{12} cm^{-3}, suggesting that the conversion efficiency of over 21% could be possibly achieved for the high-quality CdTe films with extremely low defect densities.

As shown in Fig. 8, the open-circuit voltage and fill factor were improved with the increase of carrier density in the CdTe films due to the increase of the build-in potential. The photo-generated minority carriers away from the depletion region rely on the diffusion mechanism to be collected for the contribution to the current. With the high carrier density of CdTe films, the depletion width of the CdTe solar cells was shortened, resulting in the decrease of the short-circuit current density. The increase of open-circuit voltage and fill factor compensated the loss of the short-circuit current density for the given carrier densities in this study, and hence the conversion efficiency was still improved. The simulation results showed that the efficiency of close to 21% was achieved for the CdTe films with a carrier density of 10^{17} cm^{-3}.

With the wide-gap compounds of CdZnTe (1.45–2.4 eV) or CdMgTe (1.45–3.6 eV) formed near the back of the CdTe films, the carrier recombination at the back interface could be hindered, resulting in the improvement of open-circuit voltage without significantly sacrificing the short-circuit current density. With the band alignment of the wide-gap compounds formed near the back of CdTe films, the fill factor decreased but the conversion efficiency could be still further improved due to the increase of open-circuit voltage. In our simulation results, the efficiency of 20.5% was obtained for the CdTe solar cells incorporated the wide-gap materials near the back of the CdTe films, considering that the wide-gap materials have the similar semiconductor properties to those of CdTe.

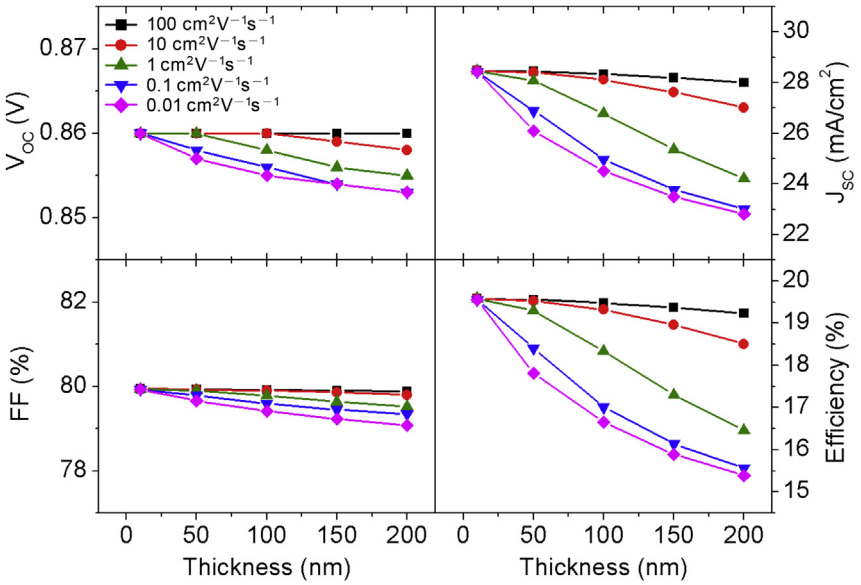

Fig. 5. Dependence of cell performance parameters on thickness of CdS films with various carrier mobilities.

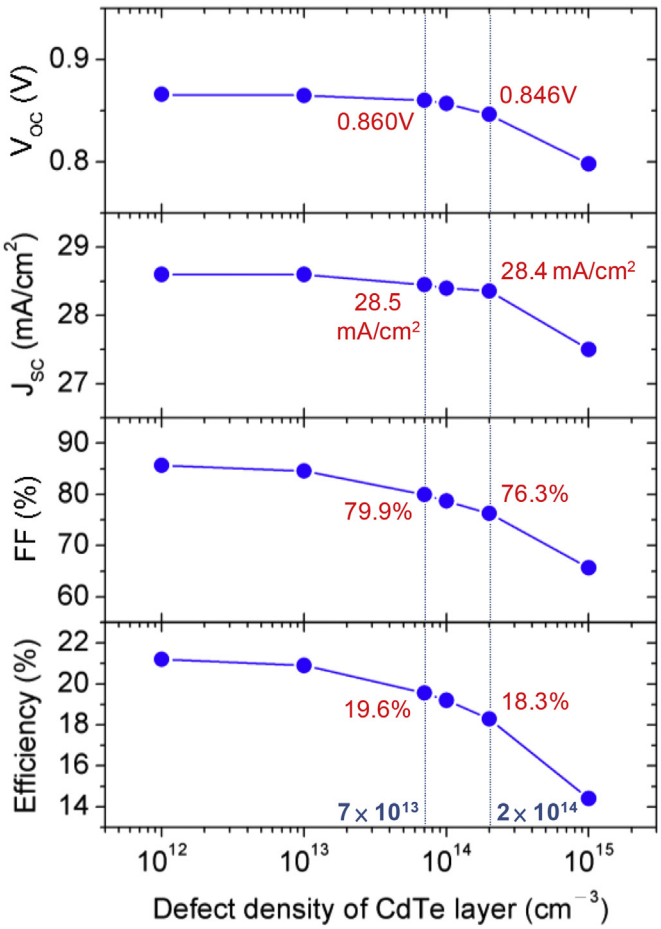

Fig. 6. Dependence of device performance on the defect density of CdTe films. (defect density: 2×10^{14} cm^{-3} and 7×10^{13} cm^{-3} for baseline and advanced models, respectively.)

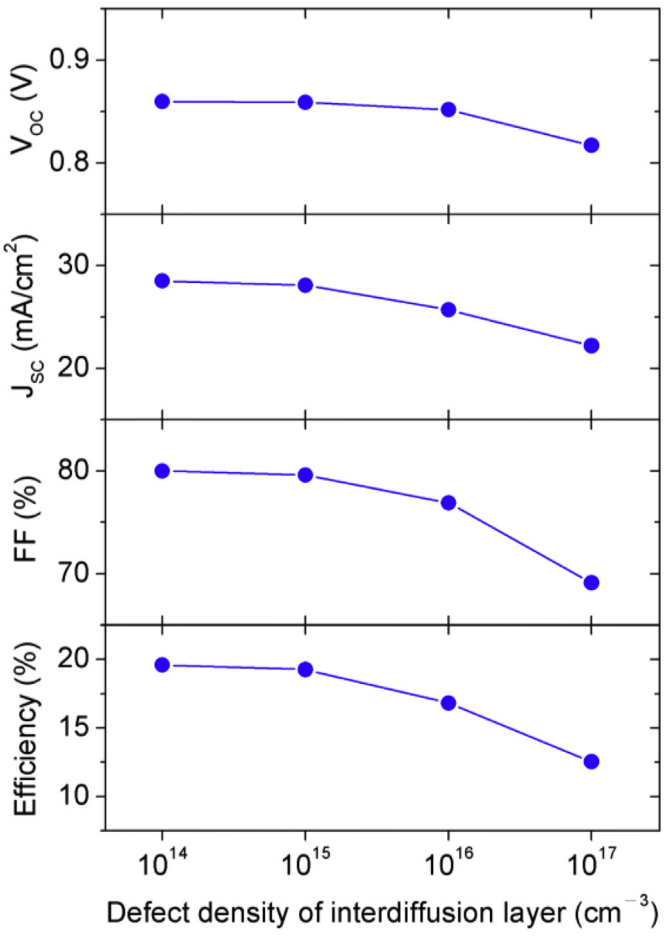

Fig. 7. Dependence of device performance on the defect density of interdiffusion layer.

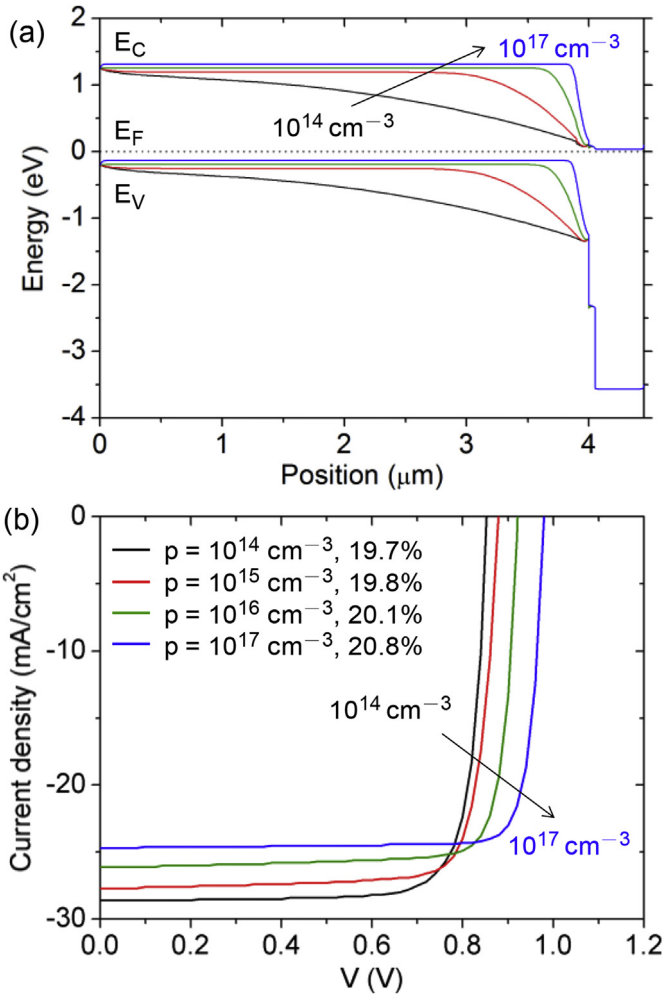

Fig. 8. (a) Schematic band diagrams of CdTe solar cells with various hole densities of CdTe films. (b) *J–V* characteristics of CdTe solar cells with various hole densities of CdTe films.

4. Summary

Device modeling and numerical simulations for the analysis of the critical semiconductor properties impacting the performance parameters of the CdTe solar cells have been conducted using the SCAPS-1D program. A baseline model and an advanced device model of CdTe solar cells with the efficiencies of 16.4% and 19.6%, respectively, were developed. In contrast to the baseline model, the improvement of performance parameters for the advanced model was analyzed. The primary contribution of the efficiency improvement was from the enhancement of the short-circuit current density, which resulted from the increase of the EQE at the wavelengths less than 520 nm. Among the properties of the CdS films, the simulation results suggested that the thickness, defect density, and carrier mobility significantly affected the short-circuit current density of the high-efficiency CdTe solar cells. The open-circuit voltage and fill factor of the CdTe solar cells were limited by the defect densities of the CdTe films and the interdiffusion layer. With the low defect densities in the CdTe films and the interdiffusion layer, the carrier recombination was repressed, and thus the open-circuit voltage and fill factor were improved. However, the short-circuit current densities of the CdTe solar cells remained constant for a wide range of defect densities in the CdTe films, and were nearly identical except for the high defect density of over 10^{15} cm^{-3}. On the contrary, the defect densities of the interdiffusion layer, which is near the surface region of the CdTe films, played a key role in affecting the short-circuit current density of the CdTe solar cells. Besides, the efficiency of CdTe solar cell could be further improved up to 20–21% for the CdTe films with the low defect density of 10^{12} cm^{-3} and the high carrier density of 10^{17} cm^{-3}, and for the incorporation of wide-gap compounds of CdZnTe or CdMgTe near the back of the CdTe films.

Acknowledgments

The authors acknowledge the use of SCAPS-1D program developed by Prof. Burgelman's group of the University of Ghent, Belgium. In addition, the authors would like to thank for the financial support of Ministry of Science and Technology (MOST), Taiwan under the contract numbers of MOST-103-2221-E-259-040.

References

[1] McCandless BE, Sites JR. Cadmium telluride solar cells. In: Luque A, Hegedus S, editors. Handbook of photovoltaic science and engineering. 2nd ed. United Kingdom: John Wiley & Sons Ltd; 2011. p. 600–41.
[2] Ohyama H, Aramoto T, Kumazawa S, Higuchi H, Arita T, Shibutani S, et al. In: Proceedings of 26th IEEE photovoltaic specialists conference, 29 Sep–3 Oct; 1997. p. 343–6. Anaheim, CA, USA.
[3] Green MA, Emery K, King DL, Igari S, Warta W. Prog Photovolt Res Appl 2001;9:287–93.
[4] Green MA, Emery K, Hishikawa Y, Warta W. Prog Photovolt Res Appl 2009;17:85–94.
[5] Green MA, Emery K, Hishikawa Y, Warta W, Dunlop ED. Prog Photovolt Res Appl 2012;20:606–14.
[6] Green MA, Emery K, Hishikawa Y, Warta W, Dunlop ED. Prog Photovolt Res Appl 2013;21:827–37.
[7] Green MA, Emery K, Hishikawa Y, Warta W, Dunlop ED. Prog Photovolt Res Appl 2014;22:701–10.
[8] Green MA, Emery K, Hishikawa Y, Warta W, Dunlop ED. Prog Photovolt Res Appl 2015;23:1–9.
[9] Sites J, Pan J. Thin Solid Films 2007;515:6099–102.
[10] Demtsu SH, Sites JR. Thin Solid Films 2006;510:320–4.
[11] Pan J, Gloeckler M, Sites JR. J Appl Phys 2006;100:124505.
[12] Niemegeers A, Burgelman M. J Appl Phys 1997;81:2881–6.
[13] Amin N, Sopian K, Konagai M. Sol Energy Mater Sol Cells 2007;91:1202–8.
[14] Hsiao K-J, Sites JR. Prog Photovolt Res Appl 2012;20:486–9.
[15] Niemegeers A, Burgelman M. In: Proceedings of 25th IEEE photovoltaic specialists conference, 13–17 May; 1996. p. 901–4. Washington, DC, USA.
[16] Burgelman M, Nollet P, Degrave S. Thin Solid Films 2000;361–362:527–32.
[17] McCandless BE, Hegedus SS. In: Proceedings of 22nd IEEE photovoltaic specialists conference, 7–11 Oct; 1991. p. 967–72. Las Vegas, NV, USA.
[18] McCandless BE, Moulton LV, Birkmire RW. Prog Photovolt Res Appl 1997;5:249–60.
[19] Agostinelli G, Bätzner DL, Burgelman M. Thin Solid Films 2003;431–432:407–13.
[20] Wei S-H, Zhang SB, Zunger A. J Appl Phys 2000;87:1304–11.
[21] Gloeckler M, Fahrenbruch AL, Sites JR. Osaka, Japan. In: Proceedings of 3rd world conference on photovoltaic energy conversion, 11–18 May; 2003. p. 491–4.
[22] Scheer R, Schock H-W. Chalcogenide photovoltaics. Germany: Wiley-VCH Verlag GmbH & Co. KGaA; 2011. p. 319.
[23] Gloeckler M, Sankin I, Zhao Z. IEEE J Photovolt 2013;3:1389–93.